2008

Preemptive vortex-loop proliferation in multicomponent interacting Bose-Einstein condensates

E. K. Dahl

E. Babaev
University of Massachusetts - Amherst, babaev1@physics.umass.edu

S. Kragset

A. Sudbo

Preemptive vortex-loop proliferation in multicomponent interacting Bose–Einstein condensates

E. K. Dahl[1], E. Babaev[2,3], S. Kragset[1], and A. Sudbø[1]
[1] *Department of Physics, Norwegian University of Science and Technology, N-7491 Trondheim, Norway*
[2] *Physics Department, University of Massachusetts, Amherst MA 01003, USA*
[3] *Department of Theoretical Physics, The Royal Institute of Technology 10691 Stockholm, Sweden*
(Dated: February 18, 2008)

We use analytical arguments and large-scale Monte Carlo calculations to investigate the nature of the phase transitions between distinct complex superfluid phases in a two-component Bose–Einstein condensate when a non-dissipative drag between the two components is being varied. We focus on understanding the role of topological defects in various phase transitions and develop vortex-matter arguments allowing an analytical description of the phase diagram. We find the behavior of fluctuation induced vortex matter to be much more complex and substantially different from that of single-component superfluids. We propose and investigate numerically a novel drag-induced "preemptive vortex loop proliferation" transition. Such a transition may be a quite generic feature in many multicomponent systems where symmetry is restored by a gas of several kinds of competing vortex loops.

PACS numbers: 03.75.Hh, 03.75.Kk, 03.75Nt, 47.32.cb

I. INTRODUCTION

Natural generalizations of many superfluid phenomena are possible in mixtures of independently conserved multicomponent Bose–Einstein condensates with intercomponent current-current interactions. The topic was first investigated in the context of $^4\mathrm{He} - {}^3\mathrm{He}$ mixtures[1,2], where it is possible to attain only a limited range of parameters. The recent progress in atomic Bose–Einstein condensates (BEC) has made it possible to access a much wider range of regimes and explore novel superfluid phases which can arise in such mixtures. For this reason, there has been much interest in a generic example of an interacting BEC mixture, namely a $U(1)\times U(1)$-symmetric system with current-current interactions. One of the novel aspects of the superfluid physics in such a system is the possibility of a phase transition at a sufficiently strong current-current interaction to a state of paired superfluid where the only broken $U(1)$ symmetry is associated with order only in the phase sum[3]. The other discussed example (which does not fall within the framework of Galilean-invariance based argument[1]) is a phase transition for bosons on an optical lattice to a state where one species of bosons pair with holes of the other species, and thereby retaining order only in the phase difference[3,4,5].

These transitions were investigated numerically in great detail in the J-current model in Ref. 6 using the worm-algorithm[7]. This numerical study, combined with mean-field arguments, revealed the interesting fact that with increasing current-current interaction, the usual second-order superfluid phase transition is altered to a first order phase transition[6]. In the free energy functional, the current-current interaction is consistent with $U(1) \times U(1)$ symmetry and the transition should therefore be associated with a proliferation of interacting vortex loops where all vortex-loop segments of the system interact with each other through a Coulomb potential. Existing theories of proliferation of such defects, however, always lead to a second-order superfluid phase transition[8]. This indicates that in this system we are faced with a novel scenario for thermally driven spontaneous vortex-loop proliferation, the detailed investigation of which is the goal of the present work.

To describe the behavior of the system undergoing these phase transitions as proliferation of vortex loops in a two-component condensate, we propose a scenario of a "preemptive vortex-loop proliferation". This scenario in particular allows us to estimate the characteristic critical couplings (or equivalently, critical temperatures) and provides a vortex-matter based picture of the transitions in the most interesting part of the phase diagram, from a state with broken $U(1)\times U(1)$ symmetry into a paired superfluid state and a subsequent transition into a normal state. To find numerical backing for the preemptive vortex-loop proliferation scenario, we perform a large-scale Monte Carlo (MC) calculation of vortex matter in the interacting BEC mixture using a representation in terms of the phases of the ordering fields of the condensates. This numerical approach allows us to study directly vortex matter and therefore may be viewed as complementary to the worm-algorithm based approach in Refs. 3,6,12. The insight which we obtain from Monte Carlo calculations on vortex matter may also shed light on how the Andreev–Bashkin effect[1] modifies the vortex-matter phase transition predicted for the liquid metallic state of hydrogen[9].

Finally, we remark that the problem of multicomponent vortex-loop proliferation has a quite generic character, since it is also related to a wide spectrum of phase transitions in other systems. An example is represented by individually conserved electrically charged condensates that communicate with each other only via a fluctuating gauge field[9,10,11,12,13,14,15]. Moreover, a related problem arises in three-dimensional generalizations of phase transitions discussed recently for certain planar spin-1 condensates[16,17].

II. THE MODEL

We consider a mixture of Bose–Einstein condensates with $U(1) \times U(1)$ symmetry and current-current interaction. This

system in the hydrodynamic limit is described by[1]

$$F = \frac{1}{2}\int_{\boldsymbol{r}} \mathrm{d}\boldsymbol{r}\left\{(\rho_1-\rho_d)\boldsymbol{v}_1^2+(\rho_2-\rho_d)\boldsymbol{v}_2^2+2\rho_d\boldsymbol{v}_1\cdot\boldsymbol{v}_2\right\}$$
$$= \frac{1}{2}\int_{\boldsymbol{r}} \mathrm{d}\boldsymbol{r}\left\{\rho_1\boldsymbol{v}_1^2+\rho_2\boldsymbol{v}_2^2-\rho_d(\boldsymbol{v}_1-\boldsymbol{v}_2)^2\right\}, \quad (1)$$

where $\boldsymbol{v}_i = \hbar\nabla\theta_i/m_i$. The last term describes a current-current interaction[1] (for its detailed microscopic derivation, see Ref. 18). The microscopic origin of the non-dissipative drag can for example be elastic inter-component scattering due to van der Waals forces between the charge-neutral atoms in the system[18], or can also originate from a lattice[3,5]. This coupling is consistent with $U(1)\times U(1)$ symmetry and thus is very different from the symmetry breaking intercomponent Josephson-coupling, which is a singular perturbation. A drag term is perturbatively irrelevant and a critical strength is needed to change the zero-drag physics of the problem, due to the extra two gradients in the coupling between the two phases.

The discrete model as such may also have a physical realization in terms of a Bose–Einstein condensate on an optical lattice[3]. In the latter case, a particularly wide range of both positive and negative ρ_d can be accessed[5]. The parameter ρ_d is a superfluid density of one condensate carried by the superfluid velocity of the other as follows from the equations of motion[1],

$$\boldsymbol{j}_1 = (\rho_1-\rho_d)\boldsymbol{v}_1+\rho_d\boldsymbol{v}_2, \quad (2)$$
$$\boldsymbol{j}_2 = (\rho_2-\rho_d)\boldsymbol{v}_2+\rho_d\boldsymbol{v}_1. \quad (3)$$

Symmetry-restoring phase transitions in this system are associated with proliferation of thermally excited topological defects, namely vortex loops[8]. In what follows, we denote vortices in the two-component condensate by a pair of integers corresponding to the winding of the phases in each of the condensates

$$(\Delta\theta_1 = 2\pi n_1, \Delta\theta_2 = 2\pi n_2) \equiv (n_1, n_2). \quad (4)$$

The current-current interaction $2\rho_d\boldsymbol{v}_1\cdot\boldsymbol{v}_2$ introduces a bias for counter-directed currents when ρ_d is positive . Indeed, this term introduces an attractive Coulomb interaction between $(\pm1,0)$ and $(0,\mp1)$ vortices. The coefficients ρ_1,ρ_2 and ρ_d must satisfy the relation

$$\rho_d < \frac{\rho_1\rho_2}{\rho_1+\rho_2}, \quad (5)$$

for stability. This puts an absolute upper bound on the amount of drag in the system that can be considered physical. In the phase diagrams to be presented below, we denote as gray (forbidden) those areas which cover the sets of parameters that violate the above inequality.

III. ENERGY SCALES ASSOCIATED WITH BARE STIFFNESSES

Let us begin by a straightforward examination of the energy scales of the problem. In what follows, we set the masses of the condensates equal and absorb $\hbar/m$ in the definition of ρ. We focus on the $\rho_d > 0$ case. In what follows, we denote expressions for phase stiffnesses for various topological excitations as $J_{(i,j)}$, (the index (i,j) refers to corresponding topological defect). The explicit expressions are given by

$$J_{(1,0)} = \rho_1-\rho_d, \quad (6)$$

$$J_{(0,1)} = \rho_2-\rho_d, \quad (7)$$

$$J_{(1,1)} = \rho_1+\rho_2, \quad (8)$$

$$J_{(1,-1)} = \rho_1+\rho_2-4\rho_d. \quad (9)$$

Let us denote the critical stiffness of the 3DXY-Villain model[19] by

$$\rho_c \approx 0.33 \quad (10)$$

Then if we neglect any interactions between different species of vortices, naive estimates of the lines where various vortex modes would proliferate, are given as follows.

$(1,0)$-vortices proliferate from an ordered background along a line defined by $\rho_1-\rho_d=\rho_c$.

$(0,1)$-vortices proliferate from an ordered background along the lines defined by $\rho_2-\rho_d=\rho_c$.

$(1,-1)$ vortices would proliferate from an ordered background along a line defined by $\rho_1+\rho_2-4\rho_d=\rho_c$.

Proliferation of $(1,1)$ is irrelevant because of the above types of topological excitations always proliferate (and thus restore symmetry) before $(1,1)$ vortices, when $\rho_d>0$.

Below we show that this naive energy-scale based picture is not correct.

IV. PHASE DIAGRAM, EQUAL STIFFNESSES

The simplest case is where the bare phase stiffnesses of each component is equal, so we begin by considering that case first.

A. Continuous phase transitions in limiting cases

The character of the vortex-loop proliferation transition can readily be understood in two limiting cases, by mapping the system to a single component model yielding standard second order phase transitions.

One limit is the trivial limit $\rho_d\to 0$, when the system is described by two independent XY models undergoing a second order phase transition from $U(1)\times U(1)$ to a symmetric state. Indeed, in this limit there is no energetic or entropic advantage in restoring order by composite topological defects.

Another limit which is fairly simple to understand, follows from the fact that by increasing ρ_d, the stiffness of $(1,-1)$-composite defects can be made arbitrarily much smaller than the stiffnesses for $(1,0)$ and $(0,1)$ defects. This is the limit

where $2\rho - 4\rho_d \approx \rho_c < (\rho - \rho_d)$ and thus the vortex loop $(1,-1)$ costs little energy to excite, while $(1,0)$ and $(0,1)$ effectively are frozen out. Physically, this also means that in this limit it is energetically costly to split a composite $(1,-1)$ defect into a pair of individual vortices, and therefore one may neglect its composite nature and map the system onto a 1-component 3DXY model undergoing a phase transition at $J_{(1,-1)} = 2\rho - 4\rho_d = \rho_c$. Because $(1,-1)$ vortices cannot disorder the phase sum, this continuous phase transition is associated with going from a $U(1) \times U(1)$ state to a state with $U(1)$ symmetry associated with order in the phase sum, which is the "paired superfluid phase" in Ref. 3.

Let us now consider the other regimes which occur in the case $\rho_1 = \rho_2 = \rho$ case. For some regimes another representation of Eq. (1) will be useful, namely

$$F = \frac{1}{2}\int_{\boldsymbol{r}} \mathrm{d}\boldsymbol{r}\Big\{\Big(\frac{\rho}{2} - \rho_d\Big)\left[\nabla(\theta_1 - \theta_2)\right]^2 + \frac{\rho}{2}\left[\nabla(\theta_1 + \theta_2)\right]^2\Big\}. \quad (11)$$

This form of the energy is particularly useful when we want to discuss the vortex matter of the remaining superfluid component in the background of proliferated composite vortices. We next proceed to discussing this situation.

B. Phase transitions in a nontrivial vortex gas background

A deviation from the vortex proliferation based on the naive energy scales scenario is manifested in the transition to a fully symmetric state in the regime $J_{(1,-1)} < J_{(1,0)} = J_{(0,1)}$, i.e. $2\rho - 4\rho_d < \rho_c < \rho - \rho_d$. To understand how this takes place, we should understand how the background of proliferated $(1,-1)$ vortices affects $(1,0)$ and $(0,1)$ vortices. This can be explained from the separation of variables in Eq. (11). The spontaneous proliferation of $(1,-1)$ vortices leaves the remaining broken symmetry only in the second term. The corresponding remaining phase stiffness is that of a "clapping mode" associated with a response to varying the phase sum. The stiffness of the clapping mode is destroyed by proliferation of the cheapest topological defects with a winding in the phase sum. These defects are individual vortices $(1,0)$ or $(0,1)$. The separation of variables Eq. (11) suggests that the background of proliferated $(1,-1)$ vortices destroys the phase stiffness in the first term and thus only the second term determines the effective stiffness of $(1,0)$ or $(0,1)$ vortices. Their stiffness is therefore reduced compared to the bare stiffness in the naive energy scale argument. The new effective stiffness is $\tilde{J}_{(1,0)} = \tilde{J}_{(1,0)} = \rho/2$, and thus it suggests that the system undergoes a phase transition to a fully symmetric state at

$$\frac{1}{2}\rho = \rho_c. \quad (12)$$

Note that from this argument, it follows that the proliferation of $(1,0)$ or $(0,1)$ vortices in the background of proliferated $(1,-1)$ vortices is determined by ρ only. This is testable in MC calculations, and we report on it below.

C. Preemptive phase transition

Now consider the most interesting regime where the line defined by the relation $J_{(1,0)} = J_{(0,1)} = \rho - \rho_d = \rho_c$ intersects the line defined by the relation $J_{(1,-1)} = 2\rho - 4\rho_d = \rho_c$. We denote the intersection point derived from the naive energy scale-based argument by $(\rho_I, \rho_{dI}) = (3\rho_c/2, \rho_c/2)$. Consider the regime slightly above the point $\rho_I = 3\rho_c/2$ (i.e. $\rho = \rho_I + \delta$ and $\rho_d = \rho_{dI} + \delta/2$). Then, from Eq. (11) we conclude that although the phase transition is indeed initiated by proliferation of the lowest-in-energy topological defects ($(1,-1)$ in this regime), the remaining stiffness for $(1,0)$ and $(0,1)$ excitations $\rho/2 \approx \rho_I/2 = 3\rho_c/4$ (which can be read off from the second term in Eq. (11)), is actually less than ρ_c. Hence, the vortices $(1,0)$ and $(0,1)$ cannot remain confined once $(1,-1)$ are proliferated. Therefore, from the separation of variables we may draw the conclusion that the simple energy-scale based picture underestimates the critical stiffnesses. More importantly, away from the limiting cases, the process is cooperative and hence proliferation of composite defects may trigger proliferation of individual vortices at a critical stiffness where arguments based on energy scales alone would predict that the individual vortex loops remain confined. Thus, with respect to $(1,0)$ and $(0,1)$ vortices, we are dealing with a "preemptive" vortex-loop proliferation scenario, triggered by the interaction with vortices in a different sector of the model. In the case where the energy of $(1,-1)$ vortices is almost the same as that of $(1,0)$ and $(0,1)$ vortices there is only one transition where by the same arguments both types of topological defects assist each other in restoring symmetry via a single phase transition. Numerical calculations which we report in the second part of this paper confirm this behavior of vortex matter. Importantly, whenever we observed this behavior, the phase transition was first order within the resolution limits of our MC calculations. The region of the phase diagram showing first order transitions in our computations, appears to be consistent with the findings in the J-current model[3] with the same symmetry, though in our case the microscopic physics is different. Note that this scenario is substantially different from the continuous loop-proliferation transition invariably encountered in a single-component model[8,19].

Fig. 1 summarizes the new estimates for the lines of vortex proliferation which follow from the separation of variable argument Eq. (11). They are given by three different regimes.

$(1,0)$- and $(0,1)$-vortices proliferate from an ordered background along a line defined by $\rho - \rho_d = \rho_c$ (solid red line in Fig. 1),

$(1,-1)$ vortices proliferate from an ordered background along a line defined by $2\rho - 4\rho_d = \rho_c$ (dashed blue line in Fig. 1),

$(1,0)$- and $(0,1)$-vortices proliferate from a background of proliferated $(1,-1)$-vortices at $\rho/2 = \rho_c$ (dashed-dotted black line in Fig. 1).

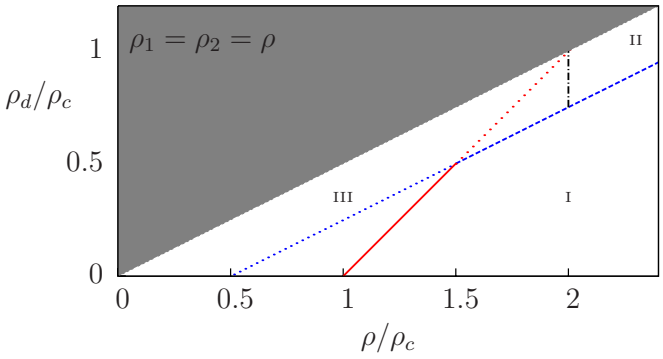

FIG. 1: (Color online) Schematic phase diagram which follows from separations of variables for the model in Eqs. (1) and (11), $\rho_1 = \rho_2 = \rho$. The gray-shaded area is the forbidden regime $\rho_d > \rho/2$. The lines separating the various regions are: a) *Solid (red) line*: Proliferation of $(1,0)$ and $(0,1)$-vortices from an ordered background (*i.e.* large ρ), along the line $\rho_d = \rho - \rho_c$. b) *Dashed (blue) line*: Proliferation of $(1,-1)$-vortices from an ordered background, along the line $\rho_d = \rho/2 - \rho_c/4$. c) *Dashed-dotted vertical (black) line*: Proliferation of $(1,0)$ and $(0,1)$-vortices from a background of proliferated $(1,-1)$-vortices, along the line $\rho = 2\rho_c$. This vortex-matter phase diagram has the same topology as that obtained from the J-current model[3]. I: $U(1) \times U(1)$; II: $U(1)$-symmetry in the phase sum; and III: a fully symmetric case.

V. PHASE DIAGRAM, UNEQUAL STIFFNESSES

We next generalize the above qualitative considerations to the case of unequal stiffnesses $\rho_1 \neq \rho_2$. We will use the notation that $\rho_2 = \alpha\rho_1; \rho_1 = \rho$. So that the coefficient α is a measure of the disparity of the stiffnesses. Since the non-triviality of the phase diagram of this model is associated with the possibility of tuning the energy of composite $(1,-1)$ defects to be less than (or comparable to) the energy of individual vortices $(1,0)$ and $(0,1)$, we use the same strategy as in the previous section to analyze this model. That is, we need to separate the variables by extracting all the stiffness terms which are *unaffected* by proliferation of $(1,-1)$ vortices. The corresponding part of the free energy functional therefore should depend on gradients of the phase sum only. Separating the variables in such a way we arrive at the following representation of the model

$$F = \frac{1}{2}\int_{\boldsymbol{r}} \mathrm{d}\boldsymbol{r}\Big\{\frac{\alpha\rho^2 - (1+\alpha)\rho\rho_d}{(1+\alpha)\rho - 4\rho_d}\left[\nabla\left(\theta_1+\theta_2\right)\right]^2 + \frac{1}{(1+\alpha)\rho - 4\rho_d}[\left(\rho - 2\rho_d\right)\nabla\theta_1 \quad -\left(\alpha\rho - 2\rho_d\right)\nabla\theta_2]^2\Big\}. \tag{13}$$

Notice the asymmetric phase weights in the second term in contrast to the symmetric separation of variables in Section IV. The asymmetry of the problem is also seen if we consider negative ρ_d which would result in decreasing the energy of $(1,1)$ vortices compared to $(1,0)$ and $(0,1)$ vortices. Negative ρ_d may be easily realized in Bose-Einstein condensates on an optical lattice, and we consider this possibility in Appendix B.

In the following qualitative discussion in this section, we consider only a positive ρ_d and without loss of generality, we assume that $\alpha > 1$. We start by going through the same energetics as we did for the case $\rho_1 = \rho_2$. First of all, the condition for stability Eq. (5), now reads $\rho_d < \alpha\rho/(1+\alpha)$. The proliferation of $(0,1)$-vortices from an ordered background is now determined by the condition $\alpha\rho - \rho_d = \rho_c$ or equivalently $\rho_d = \alpha\rho - \rho_c$ while that of $(1,0)$-vortices is determined by the condition $\rho - \rho_d = \rho_c$, or equivalently $\rho_d = \rho - \rho_c$. These lines now differ from each other, in contrast to the case $\rho_1 = \rho_2$, and hence there will be one additional region in the phase diagram. This follows, since at $\rho_d = 0$, the phase transitions in the model are expected to be two non-degenerate vortex-loop proliferation transitions in the 3DXY-universality class, with a regime with ordering only in one phase separating them. Moreover, the spontaneous proliferation of $(1,-1)$-vortices from an ordered background is now determined by the condition (to be read off from the second term in Eq. (13)) $(1+\alpha)\rho - 4\rho_d = \rho_c$ or equivalently $\rho_d = [(1+\alpha)\rho - \rho_c]/4$. These expressions reduce to those that were discussed in Section IV C for the case $\alpha = 1$.

Next, we proceed to investigate the condition for proliferation of $(0,1)$- or $(1,0)-$vortices in a background of proliferated $(1,-1)$-vortices. We thus assume (an assumption that will be checked numerically in the second part of the paper) that the coefficient of the stiffness associated with the second term in Eq. (13) has renormalized to zero. Then, the first term accounts for the only phase stiffness remaining in the system. Thus, the effective model becomes

$$F^{\mathrm{eff}}_{(1,-1)} = \frac{1}{2}\int_{\boldsymbol{r}} \mathrm{d}\boldsymbol{r}\frac{\alpha\rho^2 - (1+\alpha)\rho\rho_d}{(1+\alpha)\rho - 4\rho_d}\left[\nabla(\theta_1+\theta_2)\right]^2. \tag{14}$$

Note the rather surprising fact that, provided the composite vortices $(1,-1)$ have proliferated, the $(1,0)$- and $(0,1)$-vortices enter the effective model on equal grounds even if the bare phase stiffnesses for these differ. The origin of this fact is that $(1,-1)$ composite defects have an asymmetric effect on the partial reduction of the bare phase stiffnesses of the individual vortices. Thus $(1,0)$- or $(0,1)$ vortices will participate on equal grounds in the restoration of the remaining symmetry. Based on the above conjectures we obtain the condition for proliferation of $(1,0)$- or $(0,1)$ vortices in the background of proliferated $(1,-1)$ loops

$$\frac{\alpha\rho^2 - (1+\alpha)\rho\rho_d}{(1+\alpha)\rho - 4\rho_d} = \rho_c. \tag{15}$$

Observe that in contrast to the similar condition Eq. (12) for the case of equal stiffnesses in Section IV C, when $\alpha \neq 1$, ρ_d no longer drops out of this relation. The explicit relation is

$$\rho_d = \frac{\alpha\rho^2 - (1+\alpha)\rho\rho_c}{(1+\alpha)\rho - 4\rho_c}; \alpha \neq 1, \tag{16}$$

which is seen to approach $\rho_d \to \alpha\rho/(1+\alpha)$ from below as ρ becomes large, i.e. the proliferation line approaches the forbidden parameter region from below as $\rho \to \infty$. The

line of proliferation under discussion, namely the proliferation of $(1,0)$- and $(0,1)$-vortices in the background of proliferated $(1,-1)$-vortices, only comes into play above the dashed (blue) line separating phases I and II in Fig. 2. This is when the composite vortices are actually proliferated. We therefore only plot the line in this regime, and this is the dashed-dotted (black) line given in Fig. 2.

In Fig. 2, the solid (red) lines are the lines of proliferation of $(1,0)$- and $(0,1)$-vortices from an ordered background. At $\rho_d = 0$, they emanate linearly from $\rho = \rho_c/\alpha$ for $(1,0)$-vortices growing as $\alpha\rho$, and from $\rho = \rho_c$ for $(0,1)$-vortices growing as ρ. The dashed (blue) line represents the line of proliferation of $(1,-1)$-vortices from an ordered background. It emanates at $\rho_d = 0$ from $\rho = \rho_c/(1+\alpha)$, growing as $[(1+\alpha)\rho]/4$. The dashed-dotted (black) line represents the line across which the effective stiffness of the clapping mode $\theta_1 + \theta_2$ vanishes through the proliferation of individual vortices $(1,0)$ or $(0,1)$. The lines are seen to divide the phase diagram into four distinct regions, namely I) the completely ordered state, II) the partially ordered state with proliferated $(1,-1)$-vortices and confined individual $(1,0)$- and $(0,1)$-vortices, III) the completely disordered state with proliferated individual vortices, and IV) the partially ordered state with confined $(0,1)$-vortices and proliferated $(1,0)$-vortices. Regions II and IV are therefore two distinct partially ordered states with one broken $U(1)$-symmetry in each case.

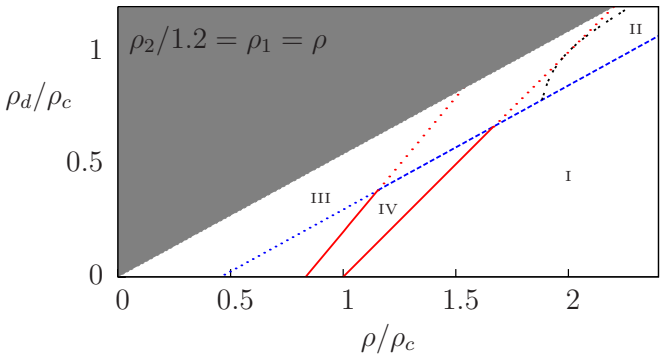

FIG. 2: (Color online) Schematic phase diagram with regions I,II, III, and IV for the model in Eqs. (1) and (13) with $\rho_2 = \alpha\rho_1 > \rho_1 = \rho$. For the purposes of illustration, we have taken $\alpha = 1.2$. The gray shaded are is the forbidden parameter regime $\rho_d > \alpha\rho/(1+\alpha)$. The lines separating the various regions are obtained as follows: a) *Solid (red) lines*: Proliferation of $(0,1)$-vortices from an ordered background, along the line $\rho_d = \alpha\rho - \rho_c$, as well as proliferation of $(0,1)$-vortices from an ordered background, along the line $\rho_d = \rho - \rho_c$. b) *Dashed (blue) line*: Proliferation of $(1,-1)$-vortices from an ordered background, along the line $\rho_d = (1+\alpha)\rho/4 - \rho_c/4$. c) *Dashed-dotted (black) line*: Line of proliferation of individual vortices $(1,0)$ or $(0,1)$ in a background of proliferated vortices $(1,-1)$, given by Eq. 16. When we cross this line from right to left, passing from region II to III, the stiffness of the clapping mode $\theta_1 + \theta_2$ is destroyed by the proliferation of individual vortices.

A. Preemptive scenario

We next discuss the preemptive scenario for vortex-loop proliferation for the more general case $\rho_1 \neq \rho_2$, largely following the line of reasoning in Section IV C. It turns out that the physics is quite rich and markedly different from the single-component case, which is rather surprising given the simplicity of the coupling term between the two condensates, cf. Eq. (1). Hence, consider the intersection point where the line of proliferation of $(1,-1)$-vortices from an ordered background is intersected by the line of proliferation of $(1,0)$-vortices from an ordered background. This intersection takes place at $(\rho_I, \rho_{dI}) = (3\rho_c/(3-\alpha), \alpha\rho_c/(3-\alpha))$. Consider now a point slightly above the intersection point above the line defined by the relation $(\rho_I + \delta, \rho_{dI} + \delta_d) = (3\rho_c/(3-\alpha) + \delta, \alpha\rho_c/(3-\alpha) + (1+\alpha)\delta/4)$, where composite vortices are proliferated. The remaining stiffness for the clapping mode, $\rho_{\rm clap}$, is given by Eq. (14)

$$\rho_{\rm clap} = \frac{\alpha\rho^2 - (1+\alpha)\rho\rho_d}{(1+\alpha)\rho - 4\rho_d}. \tag{17}$$

The question is now whether proliferation of $(1,-1)$ vortices can trigger a preemptive proliferation of $(1,0)$ and $(0,1)$ vortices. By evaluating $\rho_{\rm clap}(\rho, \rho_d, \alpha)$ at the intersection point (ρ_I, ρ_{dI}) between proliferation of individual vortices in an ordered background and proliferation of composite vortices in an ordered background, the issue is if $\rho_{\rm clap}(\rho_I, \rho_{dI}, \alpha) < \rho_c$, (*i.e.* if this estimate yields a situation that upon proliferation of composite vortices the individual vortices no longer have enough stiffness remaining to stay condensed). If this is the case, then our estimates will indicate a preemptive vortex-loop proliferation, following the same line of reasoning as was used in Section IV C (to be checked in Monte Carlo calculations in the second part of the paper).

VI. WEIGHTED PHASE SUM ORDER

It has been observed in the past that in the drag problem Eq. (1), the vortices of the type $(1,-n)$ with $n > 1$ can become energetically cheapest.[5]. Let us apply the separation of variables method to estimate analytically the position and drag dependence of the transition lines in the phase diagram when $(1,-n)$ -types of defects are relevant as well as to describe how vortex matter drives transitions from partially ordered to fully symmetric states in these cases. The accuracy of this method will be checked numerically in the second part of the paper.

Consider $\rho_2 < \rho_1$ and $\rho_d > 0$. First, one should examine for which ratio of the bare stiffnesses ρ_2/ρ_1 does the system prefer to proliferate composite $(1,-n-1)$ vortices rather then $(1,-n)$. The conditions when the energy for an $(1,-n-1)$ excitation is less then that of an $(1,-n)$ excitation can be found as follows. The phase stiffness associated with an $(1,-n)$ excitation is $J_{(1,-n)} = \rho_1 + n^2\rho_2 - (1+n)^2\rho_d$. Hence one finds that the inequality $\rho_1 + (n+1)^2\rho_2 - (n+2)^2\rho_d < \rho_1 + n^2\rho_2 - (n+1)^2\rho_d$ must be satisfied if the

system is to prefer proliferating $(1,-n-1)$ vortices in an ordered background instead of proliferating $(1,-n)$ vortices. Combined with the constraint $\rho_d < \rho_1\rho_2/(\rho_1+\rho_2)$ on ρ_d we find $\frac{2n+1}{2n+3}\rho_2 < \rho_d < \frac{\rho_1\rho_2}{\rho_1+\rho_2}$ which gives

$$\frac{\rho_2}{\rho_1} < \frac{1}{n+1/2}. \tag{18}$$

This condition is illustrated in Table I. From this, it follows that for $\rho_2/\rho_1 < 2/3$, it is energetically less costly to excite $(1,-2)$ vortices rather than $(1,-1)$ vortices for sufficiently large value of ρ_d.

TABLE I: This table shows the condition for the ratio between the bare stiffnesses, when we assume that $\rho_2 < \rho_1$ and $\rho_d > 0$, for the system to proliferate a given composite vortex.

Composite vortex	Condition
$(1,-1)$	$2/3 < \rho_2/\rho_1 < 1$
$(1,-2)$	$2/5 < \rho_2/\rho_1 < 2/3$
$(1,-3)$	$2/7 < \rho_2/\rho_1 < 2/5$
$\vdots$	$\vdots$

For such regimes the proper separation of variables is

$$F = \frac{1}{2}\int_{\boldsymbol{r}} \mathrm{d}\boldsymbol{r}\Big\{ \frac{\rho_1\rho_2 - \rho_d\left(\rho_1+\rho_2\right)}{\rho_1+n^2\rho_2-\left(1+n\right)^2\rho_d}\left(n\nabla\theta_1+\nabla\theta_2\right)^2 + \frac{1}{\rho_1+n^2\rho_2-\left(1+n\right)^2\rho_d}\Big[\left(\rho_1-(1+n)\rho_d\right)\nabla\theta_1 - \Big(\rho_2-(1+\frac{1}{n})\rho_d\Big)\nabla\theta_2\Big]^2\Big\}, \tag{19}$$

were n is an integer. This separation of variables is performed in order to extract the part of the free energy which is unaffected by $(1,-n)$ winding in the phases. Thus, upon proliferation of $(1,-n)$ vortices the system enters a phase with order in the weighted phase sum $n\theta_1+\theta_2$ (while individual phases are disordered). The effective phase stiffness which will remain in the system is given by

$$F^{\mathrm{eff}}_{(1,-n)} = \frac{1}{2}\int_{\boldsymbol{r}} \mathrm{d}\boldsymbol{r}\frac{\rho_1\rho_2-\rho_d\left(\rho_1+\rho_2\right)}{\rho_1+n^2\rho_2-\left(1+n\right)^2\rho_d}\left(n\nabla\theta_1+\nabla\theta_2\right)^2. \tag{20}$$

In contrast to the case considered in previous sections, here the individual phases do not participate on equal grounds after proliferation of $(1,-n)$ vortices because one of the phases has a factor n and is therefore more expensive to fluctuate. Nonetheless, there are several types of topological defects which can contribute on equal grounds to restore the remaining symmetry. In Fig. 3 we plot $\rho_{\mathrm{clap}}(\rho_I,\rho_{dI},\alpha)/\rho_c$ as a function of α.

For definiteness, we next consider in detail the case $n=2$. Then, the cheapest topological defect with which to restore the symmetry in Eq. (20) is given a doublet of an elementary vortex $(0,1)$ and a composite vortex $(1,-1)$ which is of lower order than the vortex $(1,-2)$ which drives the system

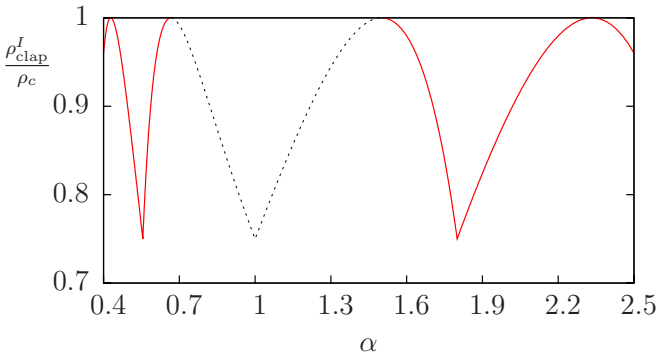

FIG. 3: (Color online) Plot of $\rho_{\mathrm{clap}}(\rho_I,\rho_{dI},\alpha)/\rho_c$ as a function of α. Note that the system is symmetric around $\alpha=1$. The dashed (black) line in the above figure shows that the remaining stiffness of the clapping mode (in the background of proliferated composite $(1,-1)$-vortices) is less than the critical coupling for vortex-loop proliferation in a parameter regime $2/3 < \alpha < 3/2$. This is the parameter regime where it is correct to limit oneself to the sector where the composite proliferated background vortices are of the type $(1,-1)$. For $\alpha < 2/3$, the composite proliferated background vortices are of type $(-n,1)$, while for $\alpha > 3/2$, the composite proliferated background vortices are of type $(1,-n)$. The fact that $\rho_{\mathrm{clap}}(\rho_I,\rho_{dI},\alpha) < \rho_c$ indicates that we are in a parameter regime where the full restoration of $U(1)\times U(1)$-symmetry proceeds from a preemptive vortex-loop proliferation phase transition, as explained in the text. The solid (red) line in the above figure shows $\rho_{\mathrm{clap}}(\rho_I,\rho_{dI},\alpha)$ for $\alpha < 2/3$ in a regime where $(2,-1)$-vortices trigger preemptive proliferation of all topological defects and $\alpha > 3/2$ where $(1,-2)$-vortices initiate the phase transition into fully symmetric state.

into the partially ordered state (20). The transition back to a fully symmetric state then takes place when

$$\frac{\rho_1\rho_2-\rho_d\left(\rho_1+\rho_2\right)}{\rho_1+n^2\rho_2-\left(1+n\right)^2\rho_d} = \rho_c. \tag{21}$$

In our MC calculations, which we report below, we check this dependence.

Before we proceed to the Monte Carlo calculations, we remark on the accuracy of the estimates of the location of the phase-transition lines based on separation of variables. The location of the phase-transition lines based on the above arguments, have corrections in the regimes of the phase diagram where several such lines split. This is because in the vicinity of such splitting points, the energy scales associated with various types of topological defects are not well separated. Hence, energetically next-to-cheapest excitations could participate in the depletion of the phase stiffness. The above arguments become more accurate as we move away from splitting points. However, they underestimate critical stiffnesses near splitting points. Below, we perform Monte Carlo simulations to study the least analytically tractable region near the splitting points. We find that even near the splitting points, the separation-of-variables based argument is quite accurate.

VII. MONTE CARLO CALCULATIONS

We next proceed to presenting our numerical results based on large-scale Monte Carlo calculations, for which we need to define our continuum model on a numerical lattice. Alternatively, we may view it as a physical realization of a 2-component Bose–Einstein condensate on an optical lattice, as alluded to above. Providing a faithful lattice representation of the continuum model Eq. (1) using phase variables is not straightforward, as some of the schemes for formulating the theory on a lattice, which are standard in the single-component case, introduce subtle artifacts when the current-current interaction between two condensates is discretize. It turns out that a study of the vortex physics in a lattice representation of the model Eq. (1) is best facilitated by the so-called Villain approximation. This accommodates the compactness of the superfluid phase of the ordering fields and accounts properly for the current-current interaction. The Villain Hamiltonian for the two-component condensate is given by

$$
\begin{aligned}
H_v\left[\boldsymbol{\Delta}\theta_1, \boldsymbol{\Delta}\theta_2\right] &= \sum_{\boldsymbol{r},\mu} V_\mu\left(\Delta_\mu\theta_1, \Delta_\mu\theta_2; T\right), \\
V_\mu(\chi_1,\chi_2;T) &= -\beta^{-1}\ln\Big\{ \sum_{n_{1,\mu},n_{2,\mu}} \mathrm{e}^{-\beta/2\left[\rho_1(\chi_1-2\pi n_{1,\mu})^2+\rho_2(\chi_2-2\pi n_{2,\mu})^2-\rho_d(\chi_1-\chi_2-2\pi(n_{1,\mu}-n_{2,\mu}))^2\right]} \Big\},
\end{aligned}
\tag{22}
$$

where the partition function of the system is given by $Z = \int_0^{2\pi} \mathcal{D}\theta_1\mathcal{D}\theta_2 \mathrm{e}^{-\beta H_v}$, and $\beta = 1/k_BT$. We have performed Monte Carlo calculations on Eq. (22), using local Metropolis updating of the fields, $\theta_1(\boldsymbol{r})$,$\theta_2(\boldsymbol{r}) \in [0, 2\pi)$, while ensuring that $\boldsymbol{\Delta}\theta_i(\boldsymbol{r}) \in [-\pi, \pi)$. The system sizes considered were $L \times L \times L$ with $L = 16, 24, 32, 40, 48, 56$ and 64. We have chosen $\beta = 1$ and varied $\rho = \rho_1 = \rho_2/\alpha$. Additionally, the drag ρ_d is chosen proportional to ρ, and thus, there is technically no difference between this approach and varying the temperature for fixed ρ, ρ_d. During the computations, we sample the total energy H_v of the system, and various helicity moduli. There are six different helicity moduli we keep track of (not all independent). The most general helicity modulus one can define in this system is applying a twist $\theta_1 \to \theta_1 + a_1\boldsymbol{r}\cdot\hat{\mathrm{e}}_\mu\delta$ and $\theta_2 \to \theta_2 + a_2\boldsymbol{r}\cdot\hat{\mathrm{e}}_\mu\delta$. The helicity modulus is then given as the second derivative of the free energy with respect to δ. For details, see Appendix A. We measure the helicity modulus associated with six different choices of twists, $(a_1 = 1, a_2 = 0)$, $(a_1 = 0, a_2 = 1)$, $(a_1 = 1, a_2 = \pm 1)$ and $(a_1 = 1, a_2 = \pm 2)$ *i.e.* twists in θ_1, θ_2, $\theta_1 \pm \theta_2$ and $\theta_1 \pm 2\theta_2$, respectively. These are denoted Υ_1^μ, Υ_2^μ, $\Upsilon_\pm^\mu$ and $\Upsilon_{1,\pm 2}^\mu$. Here, $\Upsilon_\pm^\mu = \Upsilon_1^\mu \pm 2\Upsilon_{12}^\mu + \Upsilon_2^\mu$ and $\Upsilon_{1,\pm 2}^\mu = \Upsilon_1^\mu \pm 4\Upsilon_{12}^\mu + 4\Upsilon_2^\mu$. A finite helicity modulus is a signal of a finite superfluid density of the associated quantity, a finite $\Upsilon_\pm^\mu$ represents the possibility of having co-(counter-)superflow of the two components. Likewise, the vanishing of the helicity moduli Υ_{a_1,a_2}^μ signals a thermally driven spontaneous proliferation (blowout) of vortex loops originating with multiples of 2π-windings in the phases $a_1\theta_1 + a_2\theta_2$. We have considered these quantities for equal as well as for different bare phase stiffnesses ρ_1 and ρ_2, and have in all cases varied the drag coefficient ρ_d from 0 up to the maximum allowed value compatible with the stability of the two-component superfluid ground state. The location of the phase transitions are read off from the peak in the heat capacity

We first discuss the case $\rho_1 = \rho_2$, for which results for the phase diagram and helicity moduli are shown in Fig. 4. The dotted lines represent the predictions based on our analytical arguments from the previous sections. At $\rho_d = 0$, the

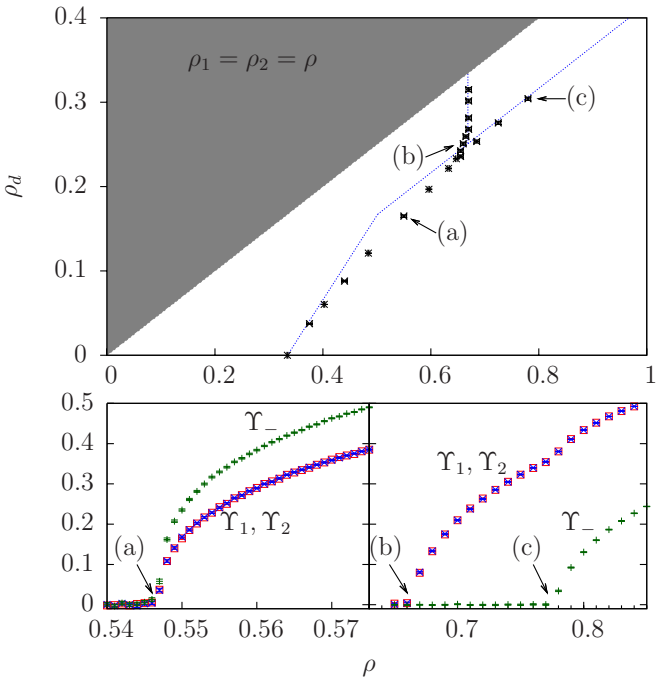

FIG. 4: (Color online) Phase diagram and a set of helicity moduli for the model Eq. (22) with equal bare stiffnesses . The shaded region illustrates the forbidden parameter regime $\rho_d > \rho/2$. The helicity moduli are Υ_1,Υ_2, and Υ_-. The leftmost helicity moduli are measured for a drag $\rho_d = 0.30\rho$, while the rightmost for $\rho_d = 0.39\rho$.

system features a doubly degenerate phase transition from a 2-component superfluid to a 2-component normal fluid at the

critical couplings $\rho_{c1} = \rho_{c2} = 0.33$. These phase transitions are in the 3DXY-universality class. When drag is introduced, it initially has the effect of reducing the stiffnesses of the individual phases θ_1 and θ_2, thus moving the doubly degenerate phase transitions to higher couplings (ρ_{1c}, ρ_{2c}). At large enough drag these phase transitions split, and the intermediate phase with ordering only in the phase sum emerges (the "paired superfluid phase" in terms of Ref. 3). We observe that our computations show that the analytic arguments advanced in previous sections describe quite accurately the phase diagram.

The line of transition from $U(1)\times U(1)$ to a fully symmetric phase changes its slope indicating that composite vortices for sufficiently large drag initiate the transition into the symmetric state (the preemptive vortex-loop proliferation scenario). Importantly, near the bending point the actual transition line is situated to the right of the dotted lines, which originate with the above bare-stiffness arguments when sub-leading type of topological defects are not taken into account. Therefore, these estimates naturally underestimate the stiffness at the actual position of a preemptive transition. However, even in this region, the deviation is not significant.

The transition line from the state with ordering only in the phase sum to a fully symmetric state precisely coincides with the analytic estimates and is independent of ρ_d, in the equal stiffnesses case, away from the splitting point. The splitting point takes place at significantly higher coupling constants in the phase diagram than what the naive energy-scale based argument gives, and is also in good agreement with the splitting point of the preemptive loops proliferation scenario discussed in Sections IV C and V A.

The corresponding results for the various helicity moduli are also shown in Fig. 4. In the lower right panel the helicity modulus Υ_- for the composite vortex mode $(1,-1)$ vanishes first as we approach lower couplings (or equivalently, higher temperatures) from the completely ordered side. The resulting state is only partially ordered. The individual stiffnesses Υ_1 and Υ_2 vanish simultaneously at some lower coupling (higher temperature), rendering the system a normal fluid. The interesting part of the phase diagram is just below the splitting point, where we have a region in which the phase transition is first-order.

We find strong indications, shown in Fig. 5, that the transition from the $U(1)\times U(1)$ state to the fully symmetric state in the region where vortex-matter based argument suggest preemptive scenario is indeed a first order transition. This is also in agreement with previous computations of the J-current model[3].

We proceed to discuss the case of slightly unequal bare stiffnesses, *i.e.* $(1,-n)$ vortices with $n > 1$ are unimportant. In our computations, we have used $\rho_2 = 1.1\rho_1$, see Fig. 6. At $\rho_d = 0$ the system features two independent phase transitions in the 3DXY-universality class at $\rho_{c1} \approx 0.33$ and $\rho_{c2} \approx 0.30$. When drag is introduced, it initially has the effect of driving the transitions to higher values of ρ (lower values of T). For moderate values of drag, these two transition close

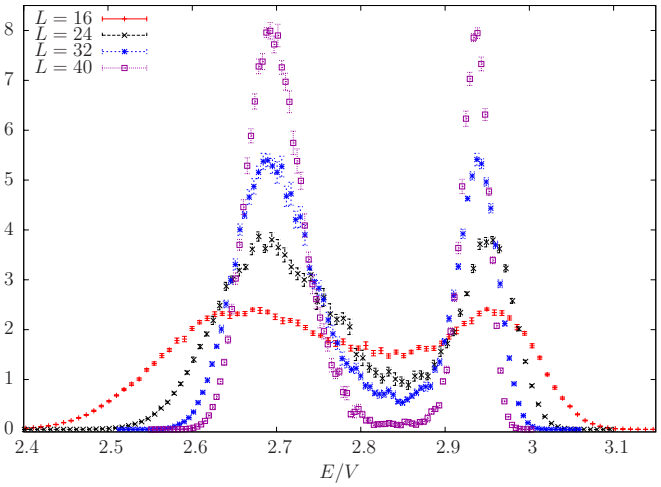

FIG. 5: (Color online) The energy histograms for $(\rho, \rho_d) \approx (0.60, 0.20)$, with $\alpha = 1$, *i.e.* in the preemptive region. A clear double peak structure is seen to develop, an indication of a first order transition. The areas under the histograms are normalized to 1.

in on each other, before they merge into one transition from a $U(1)\times U(1)$ state into the symmetric state. In terms of vortex matter, this is the preemptive region of the phase diagram. For even larger drag this line splits, and the intermediate phase with ordering associated with the phase sum emerges. The

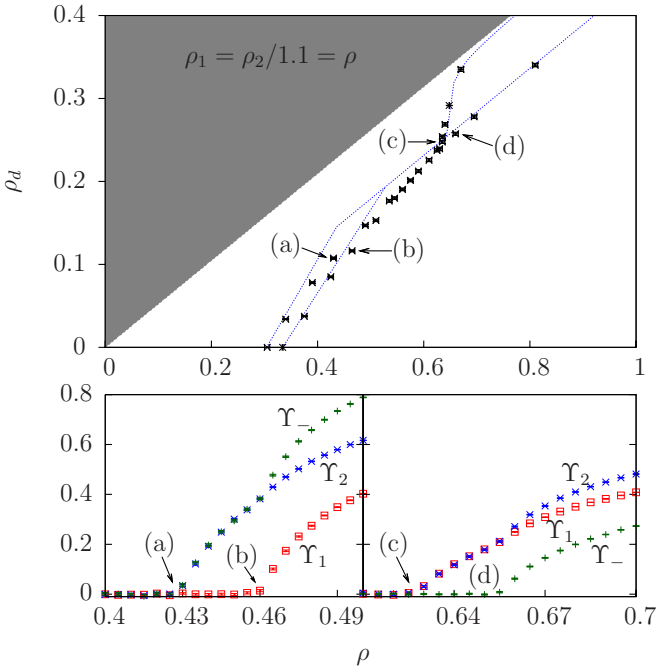

FIG. 6: (Color online) Phase diagram and a set of helicity moduli for the model Eq. (22), for $\alpha = 1.1$. The shaded region illustrates the forbidden parameter regime $\rho_d > \rho_1\rho_2/(\rho_1+\rho_2)$. The helicity moduli are Υ_1,Υ_2, and Υ_-. The left most helicity moduli are measured for a drag $\rho_d = 0.25\rho$, while the rightmost are $\rho_d = 0.39\rho$.

dotted lines in Fig. 6 are predictions described in Section V

and these agree well with our computations. Specifically, we observe that when the helicity modulus Υ_- is renormalized to zero, the individual stiffnesses become equal, as expected from our separation of variables arguments Eq. (14). Moreover, in Fig. 7, we show the corresponding energy histograms computed on the phase-transition line between points (b) and (c) in Fig. 6, namely at $(\rho, \rho_d) \approx (0.60, 0.22)$. This puts us in a part of the phase diagram where we would expect, based on our vortex-matter arguments, to be able to see the preemptive scenario explained above played out. Indeed, the phase transition is clearly seen to be of first order also in this case, thus confirming that the preemptive vortex-loop proliferation scenario is also realized for unequal bare phase stiffnesses ρ_1 and ρ_2.

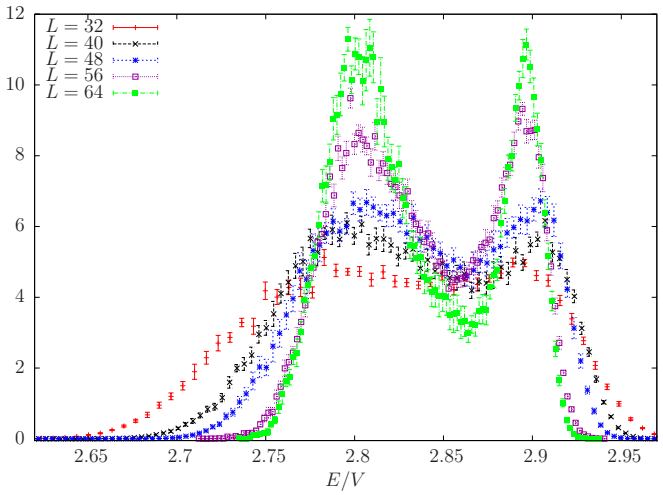

FIG. 7: (Color online) The energy histograms for $(\rho, \rho_d) \approx (0.60, 0.22)$, with $\alpha = 1.1$, i.e. in the preemptive region. A clear double peak structure is seen to develop, an indication of a first order phase transition. The areas under the histograms are normalized to 1.

We now discuss the case of significantly different bare stiffnesses, i.e. when $(1, -n)$-vortices with $n > 1$ are important. In our computation we have used $\rho_2 = 0.55\rho_1$, which from Table I indicate that we should observe a state with order in the weighted phase sum, with $n = 2$. As in the case of slightly unequal stiffnesses the system features two independent transition in the 3DXY-universality class, in our computation the transitions at $\rho_d = 0$ occurs at $\rho_{c1} \approx 0.33$ and $\rho_{c2} \approx 0.605$. At small drag values the transitions stay independent and are shifted to higher values of ρ. For moderate drag values the region with partial order (order in θ_1) becomes smaller, before disappearing at some higher drag value. The system then enters into the preemptive vortex-loop proliferation region, where the system features a transition from a $U(1) \times U(1)$-state to the fully symmetric state. In this region we find strong indications of first order transitions, shown in Fig. 9.

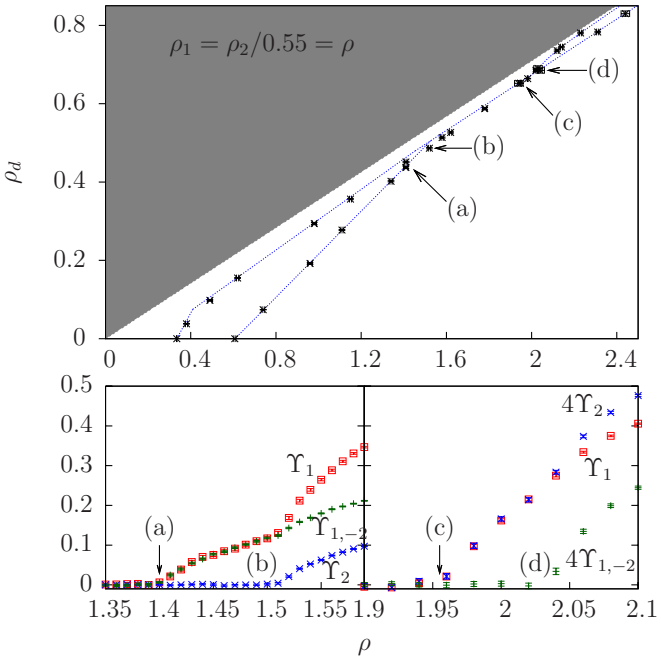

FIG. 8: (Color online) Phase diagram and a set of helicity moduli for the model Eq. (22), $\alpha = 0.55$. The shaded region illustrates the forbidden parameter regime $\rho_d > \rho_1\rho_2/(\rho_1 + \rho_2)$. The helicity moduli are Υ_1,Υ_2, and $\Upsilon_{1,-2}$. Here, the latter correspond to Υ_-, with the difference that the θ_2-phase is twisted twice as much as θ_1. The leftmost helicity moduli are measured for a drag $\rho_d = 0.32\rho$, while the rightmost are $\rho_d = 0.336\rho$.

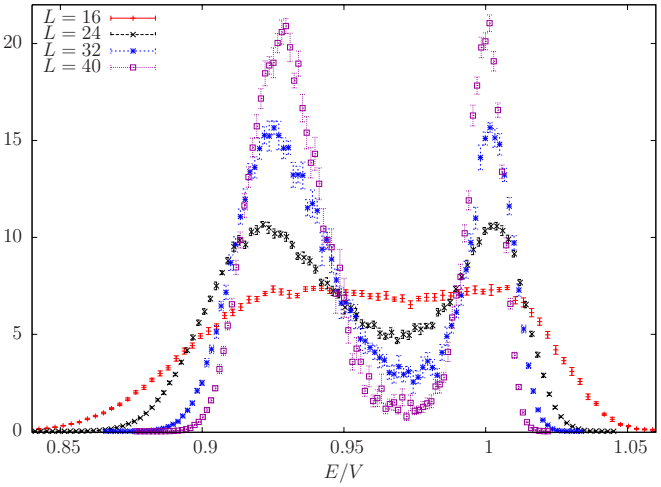

FIG. 9: (Color online) The energy histograms for $(\rho, \rho_d) \approx (1.77, 0.58)$, with $\alpha = 0.55$, i.e. in the preemptive region. A clear double peak structure is seen to develop, an indication of a first order transition. The areas under the histograms are normalized to 1.

For even larger drag values this single lines splits into two lines, and a partially ordered state appears. The partially ordered state which appears is a state were $(1, -2)$-vortices have proliferated while individual vortices stay confined (in general $(1, -n)$-vortices can proliferate). In the lower rightmost panel in Fig. 8 we observe that $\Upsilon_{1,-2}$ drops to zero while Υ_1

and Υ_2 remain finite, from this we conclude that we observe the partially ordered state with order in the weighted phase sum. The MC calculation shows that in this quite generic case that the analytical arguments from the first part of the paper are remarkably quantitatively accurate even near line-splitting points. Observe further that when $\Upsilon_{1,-2}$ have renormalized to zero we have the relation $\Upsilon_1 = 4\Upsilon_2$, as expected from the discussion near Eq. (20) (in general we expect $\Upsilon_1 = n^2\Upsilon_2$).

VIII. IMPLICATION FOR THE LIQUID METALLIC HYDROGEN PROBLEM

The approach developed above is also useful to obtain insight into the role of non-dissipative drag when it is included in the problem of multicomponent electrically charged condensates[9,10]. For example, in the problem of projected quantum fluid states of hydrogen, we deal with two electrically charged fields corresponding to electronic and protonic condensates. The fields will then be coupled by an electromagnetic gauge field in addition to the now familiar drag coupling

$$F = \frac{1}{2}\int_{\boldsymbol{r}} \mathrm{d}\boldsymbol{r}\big\{\rho\left(\nabla\theta_1 - e\boldsymbol{A}\right)^2 + \alpha\rho\left(\nabla\theta_2 + e\boldsymbol{A}\right)^2 - \rho_d\left(\nabla\theta_1 - \nabla\theta_2 - 2e\boldsymbol{A}\right)^2 + \left(\nabla\times\boldsymbol{A}\right)^2\big\}, \tag{23}$$

were e is the charge and $\boldsymbol{A}$ is the gauge field.

In this case, the physically relevant separation of variables corresponds to extraction of the phase sum. This follows, since in this situation it is the phase *sum* which is not coupled to the gauge field. This allows us to draw conclusions about superfluid and superconducting states of the system[9]. Following the same line of reasoning, an assessment of the role of non-dissipative drag is made by an extraction of the phase sum to distinguish the drastically different charged and neutral modes of the system. The model then becomes

$$F = \frac{1}{2}\int_{\boldsymbol{r}} \mathrm{d}\boldsymbol{r}\Big\{\frac{\alpha\rho^2 - (1+\alpha)\rho\rho_d}{(1+\alpha)\rho - 4\rho_d}\left[\nabla\left(\theta_1+\theta_2\right)\right]^2 + \frac{1}{(1+\alpha)\rho - 4\rho_d}\big[\left(\rho-2\rho_d\right)\nabla\theta_1 - \left(\alpha\rho - 2\rho_d\right)\nabla\theta_2 - e\{(1+\alpha)\rho - 4\rho_d\}\boldsymbol{A}\big]^2 + \left(\nabla\times\boldsymbol{A}\right)^2\Big\}. \tag{24}$$

By virtue of featuring one composite charged mode and one composite neutral mode, this model has the same structure as the model with zero drag[9,10]. However, now the stiffnesses of neutral and charged modes acquire dependence to the drag coefficient ρ_d. Therefore, the conclusions of Ref. 9 should be rather robust against finite-drag perturbations. The inter-component drag term is a quite different perturbation to the system compared to inter-component Josephson coupling. The latter is prohibited in hydrogen, but is allowed in multicomponent electronic condensates. Josephson coupling amounts to an explicit symmetry breakdown, and in terms of long length scale physics it represents a singular perturbation compared to the case where it is absent. An inter-component drag term has two gradients in it, since it is a current-current interaction. Consequently, it has a naive scaling dimension which is reduced by 2 compared to the Josephson coupling, and in contrast to the Josephson couplling it does not represent a singular perturbation. Quite the contrary, as we have seen, a critical value of the strength of the inter-component drag term is required for it to have an appreciable effect on the physics of the system.

IX. SUMMARY AND CONCLUSIONS

In this paper, we have studied the problem of the influence of non-dissipative inter-component drag on the phase diagram and phase transitions in a two-component Bose–Einstein condensate. The non-dissipative drag is a quite generic feature present in interacting multicomponent systems in the continuum as well as on a lattice[1,2,5,18]. Recently, the topology of the phase diagram and orders of the phase transitions were intensively studied in the J-current model with $U(1)\times U(1)$ symmetry by means of worm-algorithm based Monte Carlo simulations[3,4,5,6], revealing novel features such as conversions of the phase transitions from continuous to first order as a function of drag strength.

We have developed an approach in terms of topological defects for understanding these phase transitions and get new insight into physics of the various states of two-component Bose–Einstein condensates. We have carried out an investigation of the phase diagram based on analytical vortex-matter arguments, and suggested a novel scenario of vortex-matter behavior, namely a "preemptive vortex-loop proliferation". Such a scenario may well be generic to systems where symmetry is restored through proliferation of distinct topological defects in the form of vortex loops that have been excited out of the individually conserved condensates. We have found support for these scenarios in large-scale Monte Carlo calculations. These computations have been carried out using a representation of the system in terms of the phase of the complex ordering field of each of the components. The approach allows us to investigate directly the physics of topological defects in this system. Importantly, the phase representation also allows us to study the system under rotation. This can provide a bridge for studying these states of matter experimentally via rotational response. Work on this problem is in progress[20].

Acknowledgments

The authors acknowledge useful discussions with J. Hove, D. A. Huse, A. Kuklov, E.J. Mueller B. Svistunov, and M. Wallin. This work was supported by the Norwegian Research Council Grant Nos. 1585187/431, 158547/431 (NANOMAT), and Grant No. 167498/V30 (STORFORSK). The authors thank the Center for Advanced Study at the Norwegian Academy of Science and Letters, where part of this work was done.

APPENDIX A: SUPERFLUID DENSITY MATRIX IN A 2-COMPONENT SYSTEM

In general, the helicity modulus defines the superfluid density of a system. For the Andreev–Bashkin problem[1], the superfluid density is a matrix quantity given by the second derivative of the free energy of the system with respect to an infinitesimal twist in the phase, i.e. $\theta(\boldsymbol{r}) \to \theta(\boldsymbol{r}) - \boldsymbol{\delta}\cdot\boldsymbol{r}$. The helicity modulus, $\boldsymbol{\Upsilon}$, is then given as $\Upsilon_\mu = \frac{1}{L^3}\frac{\partial^2 F[\boldsymbol{\delta}]}{\partial\delta_\mu\partial\delta_\mu}\Big|_{\delta=0}$. Since $F[\boldsymbol{\delta}] = -\beta^{-1}\ln Z[\boldsymbol{\delta}]$, where β is inverse temperature and $Z[\boldsymbol{\delta}] = \int \mathcal{D}\Gamma \mathrm{e}^{-\beta H[\boldsymbol{\delta}]}$ is the partition function, the helicity modulus can further be written as

$$\Upsilon_\mu = \frac{1}{L^3}\Bigg[\left\langle\frac{\partial^2 H[\boldsymbol{\delta}]}{\partial\delta_\mu^2}\right\rangle - \beta\left\langle\left(\frac{\partial H[\boldsymbol{\delta}]}{\partial\delta_\mu} - \left\langle\frac{\partial H[\boldsymbol{\delta}]}{\partial\delta_\mu}\right\rangle\right)^2\right\rangle\Bigg]\Bigg|_{\delta=0}. \tag{A1}$$

This is a general expression for the helicity modulus, independent of the form of the Hamiltonian. We now specify the form of the Hamiltonian to that of a two-component Villain-model i.e. $H_v = \sum_{\boldsymbol{r},\nu} V_\nu(\Delta_\nu\theta_1(\boldsymbol{r}), \Delta_\nu\theta_2(\boldsymbol{r}))$ where the potential V_ν is given in Eq.(22). We now apply an arbitrary twist in the phases, $\binom{\theta_1(\boldsymbol{r})}{\theta_2(\boldsymbol{r})} \to \binom{\theta_1(\boldsymbol{r})}{\theta_2(\boldsymbol{r})} - \binom{a_1}{a_2}\boldsymbol{\delta}\cdot\boldsymbol{r}$, were a_1, a_2 are two real numbers and expressions on both side of the arrow satisfies periodic boundary conditions. The Hamiltonian then takes the form $H_v[\boldsymbol{\delta}] = \sum_{\boldsymbol{r},\nu} V_\nu(\Delta_\nu\theta_1(\boldsymbol{r}) - a_1\delta_\nu, \Delta_\nu\theta_2(\boldsymbol{r}) - a_2\delta_\nu)$. The first and second derivatives of the Hamiltonian are then given by,

$$\left.\frac{\partial H[\boldsymbol{\delta}]}{\partial\delta_\mu}\right|_{\boldsymbol{\delta}=0} = \sum_{\boldsymbol{r}}\left(-a_1\frac{\partial V_\mu}{\partial\Delta_\mu\theta_1} - a_2\frac{\partial V_\mu}{\partial\Delta_\mu\theta_2}\right) \tag{A2}$$

$$\left.\frac{\partial^2 H[\boldsymbol{\delta}]}{\partial\delta_\mu^2}\right|_{\boldsymbol{\delta}=0} = \sum_{\boldsymbol{r}}\left(a_1^2\frac{\partial^2 V_\mu}{\partial\Delta_\mu\theta_1^2} + 2a_1a_2\frac{\partial^2 V_\mu}{\partial\Delta_\mu\theta_1\partial\Delta_\mu\theta_2} + a_2^2\frac{\partial^2 V_\mu}{\partial\Delta_\mu\theta_2^2}\right). \tag{A3}$$

The helicity modulus associated with this choice of twist in the phase, is given by

$$\Upsilon^\mu_{a_1,a_2} = \frac{a_1^2}{L^3}\left[\left\langle\frac{\partial^2 H_v}{\partial\Delta_\mu\theta_1^2}\right\rangle - \beta\left\langle\left(\frac{\partial H_v}{\partial\Delta_\mu\theta_1} - \left\langle\frac{\partial H_v}{\partial\Delta_\mu\theta_1}\right\rangle\right)^2\right\rangle\right] \tag{A4}$$

$$+ \frac{2a_1a_2}{L^3}\left[\left\langle\frac{\partial^2 H_v}{\partial\Delta_\mu\theta_1\partial\Delta_\mu\theta_2}\right\rangle - \beta\left\langle\left(\frac{\partial H_v}{\partial\Delta_\mu\theta_1} - \left\langle\frac{\partial H_v}{\partial\Delta_\mu\theta_1}\right\rangle\right)\left(\frac{\partial H_v}{\partial\Delta_\mu\theta_2} - \left\langle\frac{\partial H_v}{\partial\Delta_\mu\theta_2}\right\rangle\right)\right\rangle\right] \tag{A5}$$

$$+ \frac{a_2^2}{L^3}\left[\left\langle\frac{\partial^2 H_v}{\partial\Delta_\mu\theta_2^2}\right\rangle - \beta\left\langle\left(\frac{\partial H_v}{\partial\Delta_\mu\theta_2} - \left\langle\frac{\partial H_v}{\partial\Delta_\mu\theta_2}\right\rangle\right)^2\right\rangle\right]. \tag{A6}$$

We observe that a general twist in the phases can be expressed through three independent quantities, the superfluid density of the two single components eq. (A4) and (A6), denoted Υ_1^μ and Υ_2^μ respectively, and a novel inter-component quantity Eq. (A5) denoted Υ_{12}^μ. We interpret Υ_{12} as a renormalized drag coefficient. A general helicity modulus may then be written in the compact form

$$\Upsilon^\mu_{a_1,a_2} = a_1^2\Upsilon_1^\mu + 2a_1a_2\Upsilon_{12}^\mu + a_2^2\Upsilon_2^\mu. \tag{A7}$$

APPENDIX B: NEGATIVE DRAG COEFFICIENT

The subject of the sign of the drag coefficient, ρ_d is a subtle one and depends on the physical realization of the model. In the case of a realization of the model on an optical lattice the sign of the drag coefficient can straightforwardly be made negative[5].

In the case of a negative drag coefficient the analysis in Section V will hold, with the role of $(1,1)$- and $(1,-1)$-vortices interchanged. However in the separation of variables we need to extract a phase difference to estimate the stiffness which would remain in the system when $(1,1)$ vortices proliferate. Then, the proper separation of variables for analyzing the model is given by

$$F = \int_{\boldsymbol{r}} \mathrm{d}\boldsymbol{r}\Bigg\{\left(\frac{\alpha}{1+\alpha}\rho - \rho_d\right)\left[\nabla(\theta_1-\theta_2)\right]^2 + \frac{\rho}{1+\alpha}\left[\nabla\theta_1 + \alpha\nabla\theta_2\right]^2\Bigg\}. \tag{B1}$$

[1] A. F. Andreev and E. Bashkin, Sov. Phys. JETP **42**, 164 (1975).

[2] G.E. Volovik, V. P. Mineev, and I. M. Khalatnikov, JETP **42**, 342

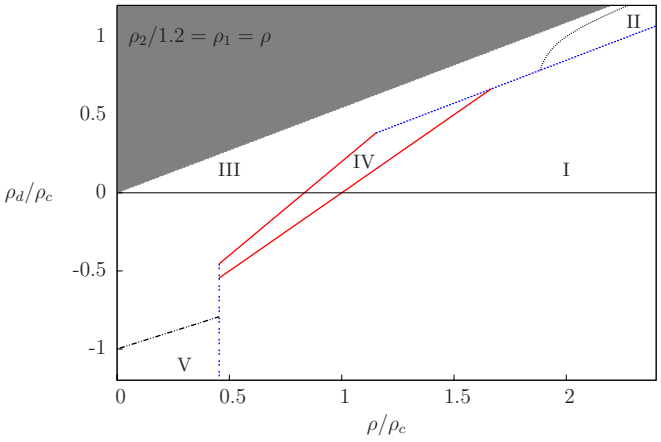

FIG. 10: (Color online) Same as Fig. 2, but now also including a negative drag coefficient ρ_d. In region I) the system features a broken $U(1) \times U(1)$ symmetry, in regions II), IV) and V) the system features a broken $U(1)$ symmetry associated with the phase sum, one individual phase and the phase difference respectively. In region III) the system is in the fully symmetric state. (See also Fig. 2).

(1975)

[3] A. Kuklov, N. Prokof'ev, and B. Svistunov, Phys. Rev. Lett. **92**, 030403 (2004).

[4] A. B. Kuklov and B. V. Svistunov, Phys. Rev. Lett. 90, 100401 (2003)

[5] V. Kaurov, A. Kuklov, and A. Meyerovich, Phys. Rev. Lett. **95**, 090403 (2005).

[6] A. Kuklov, N. Prokof'ev, and B. Svistunov, Phys. Rev. Lett. **93**, 230402 (2004).

[7] N. V. Prokof'ev, B. V. Svistunov, and I. S. Tupitsyn, Phys. Lett. A, 238 (1998); F. Alet and E. Sørensen, Phys. Rev. E **67**, 015701 (2003).

[8] C. Dasgupta and B. I. Halperin, Phys. Rev. Lett., **47** 1556 (1981); H. Kleinert, Lett. Nuovo Cimento, **35**, 409 (1982); A. K. Nguyen and A. Sudbø, Phys. Rev. B **60**, 15307 (1999); Europhys. Lett., bf 46, 780 (1999); J. Hove and A. Sudbø, Phys. Rev. Lett., **84**, 3426 (2000); J. Hove, S. Mo, and A. Sudbø, Phys. Rev. Lett., **85**, 2368 (2002).

[9] E. Babaev, A. Sudbo, and N. W. Ashcroft, Nature, **431**, 666 (2004); E. Smørgrav, J. Smiseth, E. Babaev, and A. Sudbø, Phys. Rev. Lett., **94**, 096401 (2005); *ibid* **95**, 135301 (2005); Phys. Rev. B **71**, 214509 (2005); E. Babaev and N. W. Ashcroft, Nature Physics **3**, 530 (2007).

[10] E. Babaev, Phys. Rev. Lett. **89**, 067001 (2002); Nucl. Phys. **B686**, 397 (2004).

[11] O. I. Motrunich and A. Vishwanath, Phys. Rev. B **70**, 075104 (2004).

[12] A. B. Kuklov, Prokof'ev, B. Svistunov, and M. Troyer, Ann. Phys. (N.Y.) **321**, 1602 (2006).

[13] L. Balents, L. Bartosch, A. Burkov, S. Sachdev, and K. Sengupta, Phys. Rev. B **71**, 144508 (2005).

[14] S. Kragset, F. S. Nogueira, and A. Sudbø, Phys. Rev. Lett., **97**, 170403 (2006).

[15] F. S. Nogueira, S. Kragset, and A. Sudbø, Phys. Rev. B **76**, 220403(R), (2007).

[16] E. Babaev, Phys. Rev. Lett., **94**, 137001 (2005).

[17] D. Podolsky, S. Chandrasekharan, and A.Vishwanath, `arXiv:0707.0695`, (2007). Note that in this paper, a Kosterlitz-Thouless-like transition is considered in a system with two types of *point-like topological defects*. These authors find no evidence for a first order transition, unlike in our case of two types of proliferating *vortex loops*.

[18] D. V. Fil and S. I. Shevchenko, Phys. Rev. A **72**, 013616 (2005).

[19] A. K. Nguyen and A. Sudbø, Phys. Rev. B **57**, 3123 (1998).

[20] E. K. Dahl, E. Babaev, and A. Sudbø, in preparation.